

## Quintic $G^2$ -splines for trajectory planning of autonomous vehicles

Aurelio PIAZZI and Corrado GUARINO LO BIANCO

Dipartimento di Ingegneria dell'Informazione

Università di Parma

I-43100 Parma, ITALY

aurelio@ce.unipr.it guarino@ce.unipr.it

### Abstract

*This paper presents a new motion planning primitive for car-like vehicles. It is a completely parametrized quintic spline, denoted as  $\eta$ -spline, that allows interpolating an arbitrary sequence of points with overall second order geometric ( $G^2$ -) continuity. Issues such as minimality, regularity, symmetry, and flexibility of these  $G^2$ -splines are addressed in the exposition. The development of the new primitive is tightly connected to the flatness based control of nonholonomic car-like vehicles.*

### 1 Introduction

The motion planning problem for car-like vehicles or, in general, nonholonomic systems has stimulated a significant variety of research contributions [7, 8, 10]. To cite just a few approaches we have Lie-algebraic techniques, geometric phases methods, control input parametrizations, and optimal planning (a survey reviewing motion planning methodologies with extensive bibliography is [7]). Another planning technique is the differential flatness approach of Fliess, Lévine, and coworkers [5, 4]. In particular Rouchon *et al.* [12, 11] for a car with multiple trailers showed how to obtain an open-loop control input starting with an appropriate trajectory planning on the so-called flat output. A distinguished feature of this approach that requires the flatness property of the relevant system is the obtaining of the input function through derivation (till a finite order) of the output without involving any integration. Pursuing a flatness control approach for an autonomous front-wheel driving vehicle we focus on a Cartesian trajectory planning and derive a new motion planning primitive called  $\eta$ -spline. It is a completely parametrized quintic spline that allows interpolating an arbitrary sequence of points while guaranteeing an overall second order geometric ( $G^2$ -)continuity.

Paper's organization. Section 2 describes the flatness approach for the car-like model (1) and motivates the posed polynomial  $G^2$ -interpolating problem. The quintic  $G^2$ -splines are derived in Section 3 reporting the main result

(Proposition 2), an evidence for minimality (Property 1) and a regularity result (Property 2). Section 4 investigates line generation (Property 3) and the symmetry of the  $\eta$ -parametrization (Property 4). Section 5 ends the paper with concluding remarks.

Notation. A curve on the  $\{x, y\}$ -plane can be described by a parametrization  $\mathbf{p}(u) = [x(u) \ y(u)]^T$  with real parameter  $u \in [u_0, u_1]$ . The associated "path" is the image of  $[u_0, u_1]$  under the vectorial function  $\mathbf{p}(u)$ . We say that the curve  $\mathbf{p}(u)$  is regular if there exists  $\dot{\mathbf{p}}(u)$  over  $[u_0, u_1]$  and  $\dot{\mathbf{p}}(u) \neq 0 \ \forall u \in [u_0, u_1]$ . The Euclidean norm of a vector  $\mathbf{p}$  is denoted with  $\|\mathbf{p}\|$ .

### 2 Motivation of the problem

We consider as a motion model of a vehicle the following simplified nonholonomic system:

$$\begin{cases} \dot{x} = v \cos \theta \\ \dot{y} = v \sin \theta \\ \dot{\theta} = \frac{v}{l} \tan \delta \end{cases} \quad (1)$$

where (see fig. 1)  $x$  and  $y$  are the Cartesian coordinates of the rear axle midpoint,  $v$  is the velocity of this midpoint (to be considered constant),  $\theta$  is the vehicle's heading angle,  $l$  is the inter-axle distance, and  $\delta$ , the front wheel angle, is the control variable to steer the vehicle.

The general aim is the vehicle's motion control using a differential flatness approach to be used with a road sensing systems, for example a vision-based one[2]. As known, with a flat system such as (1), a suitable trajectory planning on the system output space is the basis for deriving, by means of a dynamic inversion, the open-loop control action[5]. In a complete control scheme a feedback action may be inserted to reduce disturbances and modeling errors[9].

Now introduce the following definitions.

**Definition 1** ( $G^1$ - and  $G^2$ -curves[1]) A parametric curve  $\mathbf{p}(u)$  has first order geometric continuity and we say  $\mathbf{p}(u)$  is a  $G^1$ -curve if  $\mathbf{p}(u)$  is regular and its unit tangent vector

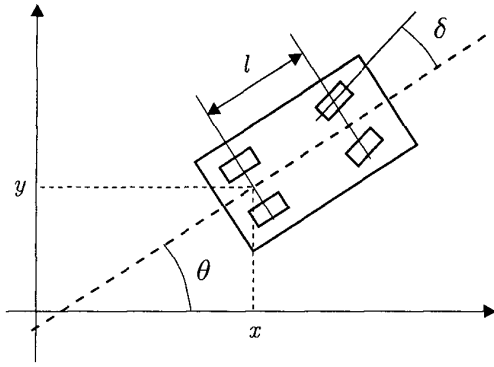


Figure 1: Vehicle's variables of the model (1).

is a continuous function along the curve. The curve  $\mathbf{p}(u)$  has second order geometric continuity and we say  $\mathbf{p}(u)$  is a  $G^2$ -curve if  $\mathbf{p}(u)$  is a  $G^1$ -curve and its curvature vector is continuous along the curve.

**Definition 2** ( $G^1$ - and  $G^2$ -paths) A path of an Euclidean space, i.e. a set of points of this space, is a  $G^i$ -path ( $i = 1, 2$ ) if there exists a parametric  $G^i$ -curve whose image is the given path.

A basic result on the vehicle's motion of model (1) is the following one, originally presented in [3].

**Proposition 1** A path on plane  $\{x, y\}$  is generated by vehicle model (1) via a continuous control input  $\delta(t)$  if and only if the  $\{x, y\}$ -path is a  $G^2$ -path.

From a control viewpoint the main consequence of the above proposition, by virtue of the flatness of (1), can be described as follows. Given any  $G^2$ -curve  $\mathbf{p}(u)$  with  $u \in [u_0, u_1]$  introduce the arc length function

$$s(u) := \int_{u_0}^u \sqrt{\dot{x}(v)^2 + \dot{y}(v)^2} dv \quad (2)$$

and denote by  $s^{-1} : [0, s(u_1)] \rightarrow [u_0, u_1]$  its inverse function. Associated with every point of  $\mathbf{p}(u)$  there is the orthonormal frame  $\{\mathbf{e}_1(u), \mathbf{e}_2(u)\}$  that is oriented in the same way of axes  $\{x, y\}$  and where  $\mathbf{e}_1(u)$  is the unit tangent vector of the curve  $\mathbf{p}(u)$ . From Frenet formulae, the curvature vector is  $\kappa(u)\mathbf{e}_2(u)$  where  $\kappa(u)$  is the scalar curvature with well defined sign. The function  $\kappa(u)$  is continuous over  $[u_0, u_1]$  because  $\mathbf{p}(u)$  is a  $G^2$ -curve. At the initial time  $t_0$ , consider the vector state of model (1) be given by  $[x(u_0) \ y(u_0) \ \arg(\mathbf{e}_1(u_0))]^T$ . Then, applying the continuous input

$$\delta(t) = \arctan[l\kappa(s^{-1}(v(t - t_0)))], \quad (3)$$

the vehicle's motion from  $t_0$  to  $t_0 + s(u_1)/v$  exactly matches the path of the given  $\mathbf{p}(u)$  curve.

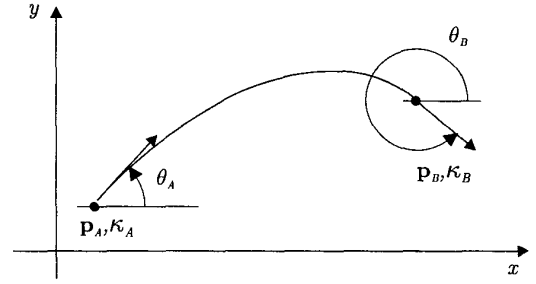


Figure 2: The  $G^2$ -interpolating problem on the  $\{x, y\}$ -plane.

Consider a sequence of Cartesian points  $\mathbf{p}_0, \mathbf{p}_1, \mathbf{p}_2, \dots$  on the  $\{x, y\}$  plane. If a piecewise curve interpolating these points can be constructed with the requirement of being an overall  $G^2$ -curve, then, using the flat dynamic inversion control given by (3), the vehicle can be steered to exactly intersect the points of the sequence. Focusing on an autonomous context, the points can be iteratively determined on the road scene by means of a vision-based sensing system using a straightforward supervisory scheme[3]. Hence, it appears naturally to pose the following problem.

*The polynomial  $G^2$ -interpolating problem:* Determine the minimal order polynomial curve that interpolates between given points  $\mathbf{p}_A = [x_A \ y_A]^T$  and  $\mathbf{p}_B = [x_B \ y_B]^T$  with associated unit tangent vectors defined by angles  $\theta_A$  and  $\theta_B$  and scalar curvatures  $\kappa_A$  and  $\kappa_B$  (see fig. 2). The signs of  $\kappa_A$  and  $\kappa_B$  are in accordance to the Frenet formulae and all the interpolating data  $\mathbf{p}_A, \mathbf{p}_B \in \mathbb{R}^2$ ,  $\theta_A, \theta_B \in [0, 2\pi)$ , and  $\kappa_A, \kappa_B \in \mathbb{R}$  can be arbitrarily assigned.

The data  $\mathbf{p}_A$ ,  $\theta_A$ , and  $\kappa_A$  may represent the vehicle's current status at time  $t_A$ , i.e. the coordinates  $x_A$  and  $y_A$  of the rear axle midpoint, the heading angle, and the curvature given by

$$\kappa_A = (1/l) \tan \delta(t_A) \quad (4)$$

where  $\delta(t_A)$  is the current steering angle. The data  $\mathbf{p}_B$ ,  $\theta_B$ , and  $\kappa_B$  may be the desired future status of the vehicle[3].

### 3 Quintic $G^2$ -splines

To solve the posed interpolating problem, consider a quintic polynomial curve  $\mathbf{p}(u) = [x(u) \ y(u)]^T$ ,  $u \in [0, 1]$  where

$$x(u) := x_0 + x_1 u + x_2 u^2 + x_3 u^3 + x_4 u^4 + x_5 u^5 \quad (5)$$

$$y(u) := y_0 + y_1 u + y_2 u^2 + y_3 u^3 + y_4 u^4 + y_5 u^5. \quad (6)$$

The interpolating conditions are the following:

$$\mathbf{p}(0) = \mathbf{p}_A, \quad \mathbf{p}(1) = \mathbf{p}_B, \quad (7)$$

$$\mathbf{e}_1(0) = \begin{bmatrix} \cos \theta_A \\ \sin \theta_A \end{bmatrix}, \quad \mathbf{e}_1(1) = \begin{bmatrix} \cos \theta_B \\ \sin \theta_B \end{bmatrix}, \quad (8)$$

$$\kappa(0) = \kappa_A, \quad \kappa(1) = \kappa_B. \quad (9)$$

where the unit tangent vector  $\mathbf{e}_1(u)$  is given by  $\dot{\mathbf{p}}(u)/\|\dot{\mathbf{p}}(u)\|$ . The quintic polynomial curve satisfying all the above conditions can be expressed as follows:

$$x_0 = x_A \quad (10)$$

$$x_1 = \eta_1 \cos \theta_A \quad (11)$$

$$x_2 = \frac{1}{2} (\eta_3 \cos \theta_A - \eta_1^2 \kappa_A \sin \theta_A) \quad (12)$$

$$x_3 = 10(x_B - x_A) - (6\eta_1 + \frac{3}{2}\eta_3) \cos \theta_A - (4\eta_2 - \frac{1}{2}\eta_4) \cos \theta_B + \frac{3}{2}\eta_1^2 \kappa_A \sin \theta_A - \frac{1}{2}\eta_2^2 \kappa_B \sin \theta_B \quad (13)$$

$$x_4 = -15(x_B - x_A) + (8\eta_1 + \frac{3}{2}\eta_3) \cos \theta_A + (7\eta_2 - \eta_4) \cos \theta_B - \frac{3}{2}\eta_1^2 \kappa_A \sin \theta_A + \eta_2^2 \kappa_B \sin \theta_B \quad (14)$$

$$x_5 = 6(x_B - x_A) - (3\eta_1 + \frac{1}{2}\eta_3) \cos \theta_A - (3\eta_2 - \frac{1}{2}\eta_4) \cos \theta_B + \frac{1}{2}\eta_1^2 \kappa_A \sin \theta_A - \frac{1}{2}\eta_2^2 \kappa_B \sin \theta_B \quad (15)$$

$$y_0 = y_A \quad (16)$$

$$y_1 = \eta_1 \sin \theta_A \quad (17)$$

$$y_2 = \frac{1}{2} (\eta_3 \sin \theta_A + \eta_1^2 \kappa_A \cos \theta_A) \quad (18)$$

$$y_3 = 10(y_B - y_A) - (6\eta_1 + \frac{3}{2}\eta_3) \sin \theta_A - (4\eta_2 - \frac{1}{2}\eta_4) \sin \theta_B - \frac{3}{2}\eta_1^2 \kappa_A \cos \theta_A + \frac{1}{2}\eta_2^2 \kappa_B \cos \theta_B \quad (19)$$

$$y_4 = -15(y_B - y_A) + (8\eta_1 + \frac{3}{2}\eta_3) \sin \theta_A + (7\eta_2 - \eta_4) \sin \theta_B + \frac{3}{2}\eta_1^2 \kappa_A \cos \theta_A - \eta_2^2 \kappa_B \cos \theta_B \quad (20)$$

$$y_5 = 6(y_B - y_A) - (3\eta_1 + \frac{1}{2}\eta_3) \sin \theta_A - (3\eta_2 - \frac{1}{2}\eta_4) \sin \theta_B - \frac{1}{2}\eta_1^2 \kappa_A \cos \theta_A + \frac{1}{2}\eta_2^2 \kappa_B \cos \theta_B \quad (21)$$

The real parameters  $\eta_i$ ,  $i = 1, \dots, 4$ , appearing in expressions (10)-(21) can be packed together to form the four-dimensional parameter vector  $\boldsymbol{\eta} := [\eta_1 \eta_2 \eta_3 \eta_4]^T$  so that the resulting parametric curve be concisely denoted as  $\mathbf{p}(u; \boldsymbol{\eta})$  or, informally,  $\boldsymbol{\eta}$ -spline. Moreover, denote with  $\mathcal{H}$  the set

given by the Cartesian product  $\mathbb{R}^+ \times \mathbb{R}^+ \times \mathbb{R} \times \mathbb{R}$ . It follows the main finding of the section.

**Proposition 2** *Given any interpolating data  $\mathbf{p}_A$ ,  $\theta_A$ ,  $\kappa_A$  and  $\mathbf{p}_B$ ,  $\theta_B$ ,  $\kappa_B$ , the parametric curve  $\mathbf{p}(u; \boldsymbol{\eta})$  satisfies conditions (7)–(9) for all  $\boldsymbol{\eta} \in \mathcal{H}$ . Conversely, given any quintic polynomial curve  $\mathbf{p}(u)$  with  $\dot{\mathbf{p}}(0) \neq 0$ ,  $\dot{\mathbf{p}}(1) \neq 0$  satisfying (7)–(9) there exists a parameter vector  $\boldsymbol{\eta} \in \mathcal{H}$  such that the quintic curve can be expressed as  $\mathbf{p}(u; \boldsymbol{\eta})$ .*

The following lemma whose proof is omitted for brevity is useful in proving the above proposition.

**Lemma 1** *Let be given any planar curve  $\mathbf{p}(u) = [x(u) \ y(u)]^T$ . Then the scalar curvature  $\kappa(u)$  is given by*

$$\kappa(u) = \frac{\dot{x}(u)\ddot{y}(u) - \ddot{x}(u)\dot{y}(u)}{(\dot{x}(u)^2 + \dot{y}(u)^2)^{3/2}}. \quad (22)$$

*Proof of Proposition 2. Sufficiency:* It can be proved by direct computations. Indeed note that  $\mathbf{p}(0; \boldsymbol{\eta}) = \mathbf{p}_A$  and  $\mathbf{p}(1; \boldsymbol{\eta}) = \mathbf{p}_B$  for all  $\boldsymbol{\eta} \in \mathcal{H}$ . Moreover, the following relations hold for all  $\boldsymbol{\eta} \in \mathcal{H}$ :

$$\dot{\mathbf{p}}(0; \boldsymbol{\eta}) = \eta_1 [\cos \theta_A \ \sin \theta_A]^T, \quad (23)$$

$$\dot{\mathbf{p}}(1; \boldsymbol{\eta}) = \eta_2 [\cos \theta_B \ \sin \theta_B]^T. \quad (24)$$

Taking into account that  $\eta_1$  and  $\eta_2$  are strictly positive we have  $\eta_1 = \|\dot{\mathbf{p}}(0; \boldsymbol{\eta})\|$  and  $\eta_2 = \|\dot{\mathbf{p}}(1; \boldsymbol{\eta})\|$  so that we derive for all  $\boldsymbol{\eta} \in \mathcal{H}$  (conditions (8)):

$$\dot{\mathbf{p}}(0; \boldsymbol{\eta}) / \|\dot{\mathbf{p}}(0; \boldsymbol{\eta})\| = [\cos \theta_A \ \sin \theta_A]^T, \quad (25)$$

$$\dot{\mathbf{p}}(1; \boldsymbol{\eta}) / \|\dot{\mathbf{p}}(1; \boldsymbol{\eta})\| = [\cos \theta_B \ \sin \theta_B]^T. \quad (26)$$

Finally, using the Cartesian expression (22) for the curvature we arrive at  $\kappa(0, \boldsymbol{\eta}) = \kappa_A$  and  $\kappa(1, \boldsymbol{\eta}) = \kappa_B$  for all  $\boldsymbol{\eta} \in \mathcal{H}$ .

*Necessity:* From conditions (7) we derive  $x_0 = x_A$ ,  $y_0 = y_A$ , i.e. relations (10) and (16), and the equations

$$x_1 + x_2 + x_3 + x_4 + x_5 = x_B - x_A, \quad (27)$$

$$y_1 + y_2 + y_3 + y_4 + y_5 = y_B - y_A. \quad (28)$$

Define

$$\eta_1 := \|\dot{\mathbf{p}}(0)\|, \ \eta_2 := \|\dot{\mathbf{p}}(1)\|, \quad (29)$$

and from the first of conditions (8) we deduce  $x_1 = \eta_1 \cos \theta_A$  and  $y_1 = \eta_1 \sin \theta_A$ , i.e. relations (11) and (17) respectively. Analogously, the equations

$$2x_2 + 3x_3 + 4x_4 + 5x_5 = \eta_2 \cos \theta_B - \eta_1 \cos \theta_A, \quad (30)$$

$$2y_2 + 3y_3 + 4y_4 + 5y_5 = \eta_2 \sin \theta_B - \eta_1 \sin \theta_A. \quad (31)$$

follow from the second of conditions (8).

By virtue of Lemma 1, the condition  $\kappa(0) = \kappa_A$  is equivalent to

$$\frac{1}{\eta_1^3} [x_1 2y_2 - 2x_2 y_1] = \kappa_A \quad (32)$$

so that we infer

$$-2x_2 \sin \theta_A + 2y_2 \cos \theta_A = \eta_1^2 \kappa_A. \quad (33)$$

Analogously, condition  $\kappa(1) = \kappa_B$  can be written as

$$\frac{1}{\eta_2^3} [\dot{x}(1)(2y_2 + 6y_3 + 12y_4 + 20y_5) - (2x_2 + 6x_3 + 12x_4 + 20x_5)\dot{y}(1)] = \kappa_B,$$

and transformed in

$$-(2x_2 + 6x_3 + 12x_4 + 20x_5) \sin \theta_B + (2y_2 + 6y_3 + 12y_4 + 20y_5) \cos \theta_B = \eta_2^2 \kappa_B \quad (34)$$

Now introduce the real parameters  $\eta_3$  and  $\eta_4$  defined as

$$\eta_3 := 2x_2 \cos \theta_A + 2y_2 \sin \theta_A, \quad (35)$$

$$\eta_4 := (2x_2 + 6x_3 + 12x_4 + 20x_5) \cos \theta_B + (2y_2 + 6y_3 + 12y_4 + 20y_5) \sin \theta_B. \quad (36)$$

Equation (33) and definition (35) permit finding relations (12) and (18):

$$\begin{aligned} x_2 &= \frac{1}{2} (\eta_3 \cos \theta_A - \eta_1^2 \kappa_A \sin \theta_A), \\ y_2 &= \frac{1}{2} (\eta_3 \sin \theta_A + \eta_1^2 \kappa_A \cos \theta_A). \end{aligned}$$

In a similar way, from equation (34) and the definition of  $\eta_4$  determine

$$2x_2 + 6x_3 + 12x_4 + 20x_5 = \eta_4 \cos \theta_B - \eta_2^2 \kappa_B \sin \theta_B, \quad (37)$$

$$2y_2 + 6y_3 + 12y_4 + 20y_5 = \eta_4 \sin \theta_B + \eta_2^2 \kappa_B \cos \theta_B. \quad (38)$$

From (27), (30), and (37) we obtain the linear equation system

$$\begin{cases} x_3 + x_4 + x_5 = x_B - x_A - x_1 - x_2 \\ 3x_3 + 4x_4 + 5x_5 = \eta_2 \cos \theta_B - \eta_1 \cos \theta_A - 2x_2 \\ 6x_3 + 12x_4 + 20x_5 = \eta_4 \cos \theta_B - \eta_2^2 \kappa_B \sin \theta_B - 2x_2 \end{cases}$$

The above system admits an unique solution in the unknowns  $x_3$ ,  $x_4$ , and  $x_5$ . After some computations and using the already found expressions for  $x_1$  and  $x_2$  we establish the relations (13), (14), and (15). Analogously, considering (28), (31), and (38) we arrive at the following system:

$$\begin{cases} y_3 + y_4 + y_5 = y_B - y_A - y_1 - y_2 \\ 3y_3 + 4y_4 + 5y_5 = \eta_2 \sin \theta_B - \eta_1 \sin \theta_A - 2y_2 \\ 6y_3 + 12y_4 + 20y_5 = \eta_4 \sin \theta_B + \eta_2^2 \kappa_B \cos \theta_B - 2y_2 \end{cases}$$

Again we have an unique solution in the unknowns  $y_3$ ,  $y_4$ , and  $y_5$  and using (17) and (18) the relations (19), (20), and (21) can be deduced.  $\square$

Note that (cf. (29))  $\eta_1$  and  $\eta_2$  are the "velocity" parameters at the beginning and at the end of curve whereas  $\eta_3$  and  $\eta_4$  can be described as the "twist" parameters.

**Property 1** *The curve  $\mathbf{p}(u; \boldsymbol{\eta})$  is the minimal order polynomial curve interpolating any arbitrarily given data  $\mathbf{p}_A, \mathbf{p}_B \in \mathbb{R}^2$ ,  $\theta_A, \theta_B \in [0, 2\pi)$ , and  $\kappa_A, \kappa_B \in \mathbb{R}$*

*Proof:* The argument is based on the already proven Proposition 2. This result points out that the curve  $\mathbf{p}(u; \boldsymbol{\eta})$  characterize all the polynomial curves, interpolating the given endpoint data, till to the fifth order. Hence, if a lower order polynomial curve exists this must coincide with  $\mathbf{p}(u; \boldsymbol{\eta})$  for some appropriate  $\boldsymbol{\eta} \in \mathcal{H}$ .

Consider as a particular interpolating data  $\mathbf{p}_A = [0 \ 0]^T$ ,  $\mathbf{p}_B = [100 \ 5]^T$ ,  $\theta_A = \theta_B = 0$ , and  $\kappa_A = \kappa_B = 0$ . From formulae (10)-(21) it is easy to derive

$$\begin{aligned} x(u; \boldsymbol{\eta}) &= \eta_1 t + (1/2) \eta_3 t^2 \\ &\quad + [1000 - 6\eta_1 - 4\eta_2 + (3/2)\eta_3 + (1/2)\eta_4] t^3 \\ &\quad + [-1500 + 8\eta_1 + 7\eta_2 + (3/2)\eta_3 - \eta_4] t^4 \\ &\quad + [600 - 3\eta_1 - 3\eta_2 - (1/2)\eta_3 + (1/2)\eta_4] t^5, \quad (39) \\ y(u; \boldsymbol{\eta}) &= 50u^3 - 75u^4 + 30u^5. \quad (40) \end{aligned}$$

Evidently, from (40), it is not possible to interpolate the given data with a fourth or lower order polynomial curve for any arbitrary choice of  $\boldsymbol{\eta} \in \mathcal{H}$ .  $\square$

**Property 2** *Denote with  $\mathcal{D}$  the interpolating data set (cf. the definition of the  $G^2$ -interpolating problem). The curve  $\mathbf{p}(u; \boldsymbol{\eta})$  is generically a regular curve over  $\mathcal{H} \times \mathcal{D}$ .*

*Proof:* A sketch of proof is offered. Denote with  $\mathbf{d} = [x_A \ y_A \ x_B \ y_B \ \theta_A \ \theta_B \ \kappa_A \ \kappa_B]^T \in \mathcal{D}$  the vector of the interpolating data. Hence we can more precisely redenote the  $\mathbf{p}(u; \boldsymbol{\eta})$  curve as

$$[x(u; \boldsymbol{\eta}, \mathbf{d}) \ y(u; \boldsymbol{\eta}, \mathbf{d})]^T.$$

With this notation  $\mathbf{p}(u; \boldsymbol{\eta})$  is not a regular curve if and only if there exists  $u \in [0, 1]$  satisfying the following system of fourth order polynomial equations:

$$\begin{cases} \dot{x}(u; \boldsymbol{\eta}, \mathbf{d}) = 0 \\ \dot{y}(u; \boldsymbol{\eta}, \mathbf{d}) = 0 \end{cases} \quad (41)$$

Hence, necessarily, the satisfaction of system (41) implies that the associated resultant is zero:

$$R(\boldsymbol{\eta}, \mathbf{d}) = 0. \quad (42)$$

Relation (42) defines a one-dimensional manifold on  $\mathcal{H} \times \mathcal{D}$ . This manifold has zero Lebesgue measure on  $\mathcal{H} \times \mathcal{D}$ ,

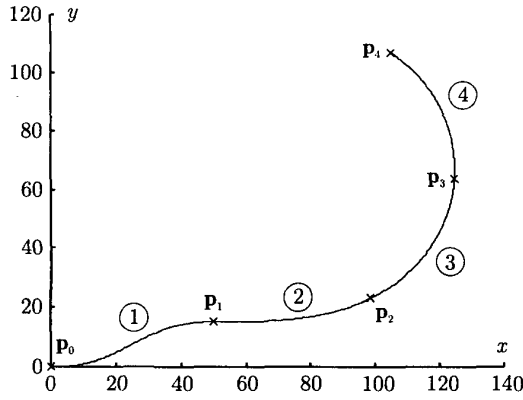


Figure 3:  $\eta$ -splines interpolating given points.

i.e.  $R(\eta, \mathbf{d})$  is generically not zero over  $\mathcal{H} \times \mathcal{D}$ . On the other hand if  $R(\eta, \mathbf{d}) \neq 0$  then the curve  $\mathbf{p}(u; \eta)$  is regular so that the statement of property 2 follows.  $\square$

Proposition 2 and Property 1 make evident that the devised  $\eta$ -spline is the solution to the posed polynomial  $G^2$ -interpolating problem. In particular Proposition 2 indicates that the  $\eta$ -spline is a complete parametrization of all fifth order polynomial curves interpolating the given endpoint data. This fact alongside the closed-form expressions (10)-(21) is very useful in performing optimal path planning [6]. On the other hand, Property 2 shows that the  $\eta$ -spline per se is generically a  $G^2$ -curve and interpolating a sequence of Cartesian points with regular  $\eta$ -splines results in an overall  $G^2$ -curve composed with quintic  $G^2$ -splines. Figure 3 exemplifies  $\eta$ -splines interpolating five points with assigned tangent angles and curvatures (see Table 1). It is apparent from the curvature plots of Figure 4 that the second spline is a good approximation of a clothoid whereas the third and fourth ones approximate circle arcs. This is somewhat remarkable in spite of having chosen just one set of  $\eta$ -parameters:  $\eta_1 = \eta_2 = 50$  and  $\eta_3 = -\eta_4 = 0$  for all the splines. Better clothoid and circle approximations as well as better lane-change curves can be obtained by choosing for each spline an optimal set of  $\eta$ -parameters [6].

#### 4 Further properties

In this section we briefly indicate two further properties of  $\eta$ -splines. The first result investigates the generation of line segments whereas the second one illustrates the inherent symmetry of the  $\eta$ -parametrization.

**Property 3** Define  $d := \|\mathbf{p}_B - \mathbf{p}_A\|$  and assume  $x_B = x_A + d \cos \theta$ ,  $y_B = y_A + d \sin \theta$ ,  $\theta_A = \theta_B = \theta \in [0, 2\pi)$ , and  $\kappa_A = \kappa_B = 0$ . Then the path generated by  $\mathbf{p}(u; \eta)$  is a segment line for any  $\eta \in \mathcal{H}$ .

Table 1: An instance of  $G^2$ -interpolating data

	$x$ [m]	$y$ [m]	$\theta$ [rad]	$k$ [m <sup>-1</sup> ]
$\mathbf{p}_0$	0	0	0	0
$\mathbf{p}_1$	50.00	15.00	0	0
$\mathbf{p}_2$	98.76	23.19	0.50	1/50
$\mathbf{p}_3$	124.67	63.53	1.50	1/50
$\mathbf{p}_4$	104.72	107.12	2.50	1/50

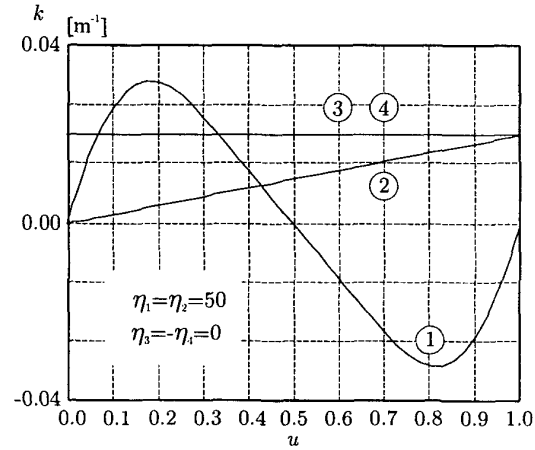


Figure 4: Plots of curvatures of the  $\eta$ -splines appearing in Figure 3.

*Proof:* Taking the property assumptions and substituting them into relations (10)-(21) we obtain:

$$\begin{aligned}
 \mathbf{p}(u; \eta) &= \begin{bmatrix} x_A \\ y_A \end{bmatrix} \\
 &+ \eta_1 \begin{bmatrix} \cos \theta \\ \sin \theta \end{bmatrix} u + \frac{1}{2} \eta_3 \begin{bmatrix} \cos \theta \\ \sin \theta \end{bmatrix} u^2 \\
 &+ (10d - 6\eta_1 - 4\eta_2 - \frac{3}{2}\eta_3 + \frac{1}{2}\eta_4) \begin{bmatrix} \cos \theta \\ \sin \theta \end{bmatrix} u^3 \\
 &+ (-15d + 8\eta_1 + 7\eta_2 + \frac{3}{2}\eta_3 - \eta_4) \begin{bmatrix} \cos \theta \\ \sin \theta \end{bmatrix} u^4 \\
 &+ (6d - 3\eta_1 - 3\eta_2 - \frac{1}{2}\eta_3 + \frac{1}{2}\eta_4) \begin{bmatrix} \cos \theta \\ \sin \theta \end{bmatrix} u^5. \quad (43)
 \end{aligned}$$

Then the  $\eta$ -spline can be rewritten as

$$\mathbf{p}(u; \eta) = \begin{bmatrix} x_A \\ y_A \end{bmatrix} + f(u; \eta) \begin{bmatrix} \cos \theta \\ \sin \theta \end{bmatrix} \quad (44)$$

with  $f(u; \eta)$  being the appropriate function. Evidently, from (44),  $\mathbf{p}(u; \eta)$  belongs to the segment line joining  $\mathbf{p}_A$

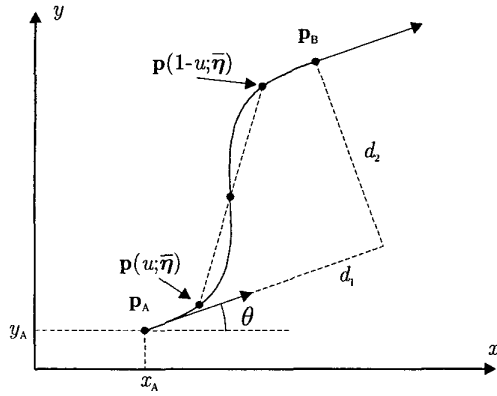


Figure 5: Symmetry in shaping a lane-change curve.

and  $p_B$  for all  $u \in [0, 1]$  and all  $\eta \in \mathcal{H}$ .  $\square$

The next result exposes a symmetry property with reference to the so-called "lane-change" curve (see Figure 5).

**Property 4** Assume  $\eta_1 = \eta_2 = v \in \mathbb{R}^+$  and  $\eta_3 = -\eta_4 = w \in \mathbb{R}$  and define  $\bar{\eta} := [v \ v \ w \ -w]^T$ . Moreover, consider  $\theta_A = \theta_B = \theta \in [0, 2\pi)$ ,  $\kappa_A = \kappa_B = 0$ , and

$$\begin{cases} x_B = x_A + d_1 \cos \theta - d_2 \sin \theta \\ y_B = y_A + d_1 \sin \theta + d_2 \cos \theta \end{cases} \quad (45)$$

where  $d_1 \in \mathbb{R}^+$  and  $d_2 \in \mathbb{R}$ . Then it follows

$$p(1-u; \bar{\eta}) = p_A + p_B - p(u; \bar{\eta}) \quad (46)$$

$\forall u \in [0, 1], \forall v \in \mathbb{R}^+, \forall w \in \mathbb{R}$

*Proof:* By direct substitution into (10)-(21) of all the posed assumptions and after some computations we have:

$$\begin{aligned} p(u; \bar{\eta}) &= \begin{bmatrix} x_A \\ y_A \end{bmatrix} + v \begin{bmatrix} \cos \theta \\ \sin \theta \end{bmatrix} u + \frac{1}{2} w \begin{bmatrix} \cos \theta \\ \sin \theta \end{bmatrix} u^2 \\ &+ \begin{bmatrix} \cos \theta & -\sin \theta \\ \sin \theta & \cos \theta \end{bmatrix} \begin{bmatrix} 10d_1 - 10v - 2w \\ 10d_2 \end{bmatrix} u^3 \\ &+ \begin{bmatrix} \cos \theta & -\sin \theta \\ \sin \theta & \cos \theta \end{bmatrix} \begin{bmatrix} -15d_1 + 15v + (5/2)w \\ -15d_2 \end{bmatrix} u^4 \\ &+ \begin{bmatrix} \cos \theta & -\sin \theta \\ \sin \theta & \cos \theta \end{bmatrix} \begin{bmatrix} 6d_1 - 6v - w \\ 6d_2 \end{bmatrix} u^5. \end{aligned} \quad (47)$$

Using the above expression (47) for  $p(u; \bar{\eta})$  we verify that relation (46) holds for all  $u \in [0, 1]$ ,  $v \in \mathbb{R}^+$ , and  $w \in \mathbb{R}$ .  $\square$

Besides symmetry, Property 4 points out the possibility of shaping the lane-change by varying the "velocity" parameter  $\eta_1 = \eta_2 = v \in \mathbb{R}^+$  and the "twist" parameter  $\eta_3 = -\eta_4 = w \in \mathbb{R}$ . This can be done in an optimal fashion as explained in [6].

## 5 Conclusions

A new motion planning primitive, i.e. the quintic  $G^2$ -spline, has been introduced. Using the shaping parameter vector  $\eta$  it is easy to obtain, or approximate, line segments, circle arcs, clothoids, and lane-change curves [6]. A promising use of the proposed splines for the motion of an autonomous vehicle can be predictively obtained by adopting a vision sensing system integrated into a flatness based control architecture [3].

## Acknowledgements.

Partial support for this research has been provided by MURST scientific research funds.

## References

- [1] B. A. Barsky and J. C. Beatty. Local control of bias and tension in beta-spline. *Computer Graphics*, 17(3):193–218, 1983.
- [2] M. Bertozzi and A. Broggi. GOLD: a parallel real-time stereo vision system for generic obstacle and lane detection. *IEEE Trans. Image Processing*, 7:62–81, Jan. 1998.
- [3] A. Broggi, M. Bertozzi, A. Fascioli, C. Guarino Lo Bianco, and A. Piazzini. The ARGO autonomous vehicle's vision and control systems. *Inter. J. of Intelligent Control and Systems*, 2000. to appear.
- [4] M. Fliess, J. Lévin, P. Martin, F. Ollivier, and P. Rouchon. Controlling nonlinear systems by flatness. In C. Byrnes, B. Datta, D. Gillian, and C. Martin, editors, *Systems and Control in the Twenty-First Century*, pages 137–154. Birkhäuser, 1997.
- [5] M. Fliess, J. Lévin, P. Martin, and P. Rouchon. Flatness and defect of nonlinear systems: introduction theory and examples. *Int. J. of Control*, 61(6):1327–1361, 1995.
- [6] C. Guarino Lo Bianco and A. Piazzini. Optimal trajectory planning with quintic  $G^2$ -splines. In *Proceedings of the IEEE Intelligent Vehicles Symposium*, Dearborn, MI, Oct. 2000.
- [7] I. Kolmanovsky and N. McClamroch. Developments in nonholonomic control problems. *IEEE Control Systems Magazine*, 15(6):21–36, Dec. 1995.
- [8] J.-C. Latombe. *Robot motion planning*. Kluwer, 1991.
- [9] J. Lévine. Are there new industrial perspectives in the control of mechanical systems? In P. M. Frank, editor, *Advances in Control: highlights of ECC'99*, pages 197–226, London, Great Britain, 1999. Springer-Verlag.
- [10] R. Murray, Z. Li, and S. Sastry. *A Mathematical Introduction to Robotic Manipulation*. CRC Press, 1994.
- [11] P. Rouchon, M. Fliess, J. Lévin, and P. Martin. Flatness and motion planning: the car with  $n$  trailers. In *Proceedings of the European Control Conference, ECC'93*, pages 1518–1522, Groninger, Netherlands, 1993.
- [12] P. Rouchon, M. Fliess, J. Lévin, and P. Martin. Flatness, motion planning and trailer systems. In *Proceedings of the 32nd IEEE Conference on Decision and Control, CDC'93*, pages 2700–2705, 1993.